

**CASE FILE  
COPY**

FILE COPY  
NO. 6

**NATIONAL ADVISORY COMMITTEE  
FOR AERONAUTICS**

**REPORT No. 730**

**AN INVESTIGATION OF THE DRAG OF WINDSHIELDS  
IN THE 8-FOOT HIGH-SPEED WIND TUNNEL**

By **RUSSELL G. ROBINSON** and **JAMES B. DELANO-**



**NASA FILE COPY**  
Loan expires on last  
date stamped on back cover.  
**PLEASE RETURN TO**  
**REPORT DISTRIBUTION SECTION**  
**LANGLEY RESEARCH CENTER**  
**NATIONAL AERONAUTICS AND**  
**SPACE ADMINISTRATION**  
Langley Field, Virginia

1942

## AERONAUTIC SYMBOLS

### 1. FUNDAMENTAL AND DERIVED UNITS

|             | Symbol   | Metric                    |                   | English                |                   |
|-------------|----------|---------------------------|-------------------|------------------------|-------------------|
|             |          | Unit                      | Abbrevia-<br>tion | Unit                   | Abbrevia-<br>tion |
| Length..... | <i>l</i> | meter.....                | m                 | foot (or mile).....    | ft (or mi)        |
| Time.....   | <i>t</i> | second.....               | s                 | second (or hour).....  | sec (or hr)       |
| Force.....  | <i>F</i> | weight of 1 kilogram..... | kg                | weight of 1 pound..... | lb                |
| Power.....  | <i>P</i> | horsepower (metric).....  |                   | horsepower.....        | hp                |
| Speed.....  | <i>V</i> | {kilometers per hour..... | kph               | miles per hour.....    | mph               |
|             |          | {meters per second.....   | mps               | feet per second.....   | fps               |

### 2. GENERAL SYMBOLS

|   |   |
|---|---|
| <p><i>W</i> Weight = <math>mg</math></p> <p><i>g</i> Standard acceleration of gravity = <math>9.80665 \text{ m/s}^2</math><br/>or <math>32.1740 \text{ ft/sec}^2</math></p> <p><i>m</i> Mass = <math>\frac{W}{g}</math></p> <p><i>I</i> Moment of inertia = <math>mk^2</math>. (Indicate axis of<br/>radius of gyration <math>k</math> by proper subscript.)</p> <p><math>\mu</math> Coefficient of viscosity</p> | <p><math>\nu</math> Kinematic viscosity</p> <p><math>\rho</math> Density (mass per unit volume)<br/>Standard density of dry air, <math>0.12497 \text{ kg-m}^{-4}\text{-s}^2</math> at <math>15^\circ \text{ C}</math><br/>and <math>760 \text{ mm}</math>; or <math>0.002378 \text{ lb-ft}^{-4} \text{ sec}^2</math><br/>Specific weight of "standard" air, <math>1.2255 \text{ kg/m}^3</math> or<br/><math>0.07651 \text{ lb/cu ft}</math></p> |
|---|---|

### 3. AERODYNAMIC SYMBOLS

|  |  |
|--|--|
| <p><i>S</i> Area</p> <p><i>S<sub>w</sub></i> Area of wing</p> <p><i>G</i> Gap</p> <p><i>b</i> Span</p> <p><i>c</i> Chord</p> <p><i>A</i> Aspect ratio, <math>\frac{b^2}{S}</math></p> <p><i>V</i> True air speed</p> <p><i>q</i> Dynamic pressure, <math>\frac{1}{2}\rho V^2</math></p> <p><i>L</i> Lift, absolute coefficient <math>C_L = \frac{L}{qS}</math></p> <p><i>D</i> Drag, absolute coefficient <math>C_D = \frac{D}{qS}</math></p> <p><i>D<sub>0</sub></i> Profile drag, absolute coefficient <math>C_{D_0} = \frac{D_0}{qS}</math></p> <p><i>D<sub>i</sub></i> Induced drag, absolute coefficient <math>C_{D_i} = \frac{D_i}{qS}</math></p> <p><i>D<sub>p</sub></i> Parasite drag, absolute coefficient <math>C_{D_p} = \frac{D_p}{qS}</math></p> <p><i>C</i> Cross-wind force, absolute coefficient <math>C_c = \frac{C}{qS}</math></p> | <p><math>i_w</math> Angle of setting of wings (relative to thrust line)</p> <p><math>i_t</math> Angle of stabilizer setting (relative to thrust<br/>line)</p> <p><i>Q</i> Resultant moment</p> <p><math>\Omega</math> Resultant angular velocity</p> <p><i>R</i> Reynolds number, <math>\rho \frac{Vl}{\mu}</math> where <math>l</math> is a linear dimen-<br/>sion (e.g., for an airfoil of 1.0 ft chord, 100 mph,<br/>standard pressure at <math>15^\circ \text{ C}</math>, the corresponding<br/>Reynolds number is 935,400; or for an airfoil<br/>of 1.0 m chord, 100 mps, the corresponding<br/>Reynolds number is 6,865,000)</p> <p><i>a</i> Angle of attack</p> <p><math>\epsilon</math> Angle of downwash</p> <p><math>a_0</math> Angle of attack, infinite aspect ratio</p> <p><math>a_i</math> Angle of attack, induced</p> <p><math>a_a</math> Angle of attack, absolute (measured from zero-<br/>lift position)</p> <p><math>\gamma</math> Flight-path angle</p> |
|--|--|

---

**REPORT No. 730**

---

**AN INVESTIGATION OF THE DRAG OF WINDSHIELDS  
IN THE 8-FOOT HIGH-SPEED WIND TUNNEL**

By **RUSSELL G. ROBINSON and JAMES B. DELANO**

**Langley Memorial Aeronautical Laboratory**

---

# NATIONAL ADVISORY COMMITTEE FOR AERONAUTICS

HEADQUARTERS, 1500 NEW HAMPSHIRE AVENUE NW., WASHINGTON, D. C.

Created by act of Congress approved March 3, 1915, for the supervision and direction of the scientific study of the problems of flight (U. S. Code, title 50, sec. 151). Its membership was increased to 15 by act approved March 2, 1929. The members are appointed by the President, and serve as such without compensation.

JEROME C. HUNSAKER, Sc. D., *Chairman*,  
Cambridge, Mass.

GEORGE J. MEAD, Sc. D., *Vice Chairman*,  
Washington, D. C.

CHARLES G. ABBOT, Sc. D.,  
Secretary, Smithsonian Institution.

HENRY H. ARNOLD, Lieut. General, United States Army,  
Commanding General, Army Air Forces, War Department.

LYMAN J. BRIGGS, Ph. D.,  
Director, National Bureau of Standards.

W. A. M. BURDEN,  
Special Assistant to the Secretary of Commerce.

VANNEVAR BUSH, Sc. D., Director,  
Office Scientific Research and Development,  
Washington, D. C.

WILLIAM F. DURAND, Ph. D.,  
Stanford University, Calif.

O. P. ECHOLS, Major General, United States Army, Com-  
manding General, The Matériel Command, Army Air  
Forces, War Department.

SYDNEY M. KRAUS, Captain, United States Navy, Bureau of  
Aeronautics, Navy Department.

FRANCIS W. REICHELDERFER, Sc. D.,  
Chief, United States Weather Bureau.

JOHN H. TOWERS, Rear Admiral, United States Navy,  
Chief, Bureau of Aeronautics, Navy Department.

EDWARD WARNER, Sc. D.,  
Civil Aeronautics Board,  
Washington, D. C.

ORVILLE WRIGHT, Sc. D.,  
Dayton, Ohio.

THEODORE P. WRIGHT, Sc. D.,  
Asst. Chief, Aircraft Branch,  
War Production Board.

GEORGE W. LEWIS, *Director of Aeronautical Research*

JOHN F. VICTORY, *Secretary*

HENRY J. E. REID, *Engineer-in-Charge, Langley Memorial Aeronautical Laboratory, Langley Field, Va.*

SMITH J. DEFRANCE, *Engineer-in-Charge, Ames Aeronautical Laboratory, Moffett Field, Calif.*

EDWARD R. SHARP, *Administrative Officer, Aircraft Engine Research Laboratory, Cleveland Airport, Cleveland, Ohio*

## TECHNICAL COMMITTEES

AERODYNAMICS  
POWER PLANTS FOR AIRCRAFT

AIRCRAFT MATERIALS  
AIRCRAFT STRUCTURES

INVENTIONS & DESIGNS  
OPERATING PROBLEMS

*Coordination of Research Needs of Military and Civil Aviation*

*Preparation of Research Programs*

*Allocation of Problems*

*Prevention of Duplication*

*Consideration of Inventions*

LANGLEY MEMORIAL AERONAUTICAL LABORATORY

LANGLEY FIELD, VA.

AMES AERONAUTICAL LABORATORY

MOFFETT FIELD, CALIF.

AIRCRAFT ENGINE RESEARCH LABORATORY

CLEVELAND AIRPORT, CLEVELAND, OHIO

Conduct, under unified control, for all agencies, of scientific research on the fundamental problems of flight

OFFICE OF AERONAUTICAL INTELLIGENCE

WASHINGTON, D. C.

Collection, classification, compilation, and dissemination of  
scientific and technical information on aeronautics

## REPORT No. 730

### AN INVESTIGATION OF THE DRAG OF WINDSHIELDS IN THE 8-FOOT HIGH-SPEED WIND TUNNEL

By RUSSELL G. ROBINSON and JAMES B. DELANO

#### SUMMARY

*The drag of closed-cockpit and transport-type windshields was determined from tests made at speeds corresponding to a Mach number range of approximately 0.25 to 0.58 in the NACA 8-foot high-speed wind tunnel. This speed range corresponds to a test Reynolds number range of 2,510,000 to 4,830,000 based on the mean aerodynamic chord of the full-span model (17.29 in.). The shapes of the windshield proper, the hood, and the tail fairing were systematically varied to include common types and a refined design. Transport types varied from a reproduction of a current type to a completely faired windshield.*

*The results show that the drag of windshields of the same frontal area, on airplanes of small to medium size, may account for 15 percent of the airplane drag or may be reduced to 1 percent. Optimum values are given for windshield and tail-fairing lengths; the effect, at various airspeeds, of rounding off sharp corners to various radii is shown. The longitudinal profile of a windshield is shown to be most important and the transverse profile, to be much less important. The effects of retaining strips, of steps for telescoping hoods, and of recessed windows are determined. The results show that the drag of transport-type windshields may account for 21 percent of the fuselage drag or may be reduced to 2 percent.*

#### INTRODUCTION

Prior to the present investigation, no comparative test results were available for obtaining the drag of windshields at high speeds. Most windshield investigations were concerned with the field of view and the adaptability of windshields to bad weather (references 1, 2, and 3). Some comparative wind-tunnel tests (reference 1), however, show the drag of a certain family of windshields; these tests were made at approximately one-fifth scale, at 82 miles per hour, and at angles of attack corresponding to maximum speed and no lift. Wind-tunnel tests reported in reference 4 show the reduction in drag obtained by modifying a given forward-sloping V-type cabin windshield.

In the present investigation, the drags of windshields of the types representative of present trends in design

for private, military, and transport airplanes were determined through a wide speed range. For the closed-cockpit types, the following geometric factors were investigated: nose shape, nose length, tail length, tail shape, transverse profile, discontinuities (retaining strips and steps for telescoping hoods), and radius of curvature at juncture of hood with nose and tail sections. In addition, surface pressures were measured at one point on a short conical nose section and at several points on a streamline nose section of medium length to serve as an indication of critical speeds and of the air loads to which windshields are subjected. The transport-type windshields included in the investigation were a reproduction of a commonly used windshield; windshields with the same glass area but utilizing flush flat panels, flush single-curved glass, and flush double-curved glass; and a design in which the windshield discontinuity was completely faired out.

These tests were conducted in the NACA 8-foot high-speed wind tunnel (reference 5) at speeds corresponding to a Mach number range of approximately 0.25 to 0.58 for fuselage angles of attack ranging from  $-3.55^\circ$  to  $0.03^\circ$  giving airplane lift coefficients from 0 to approximately 0.4, respectively. The speed range corresponds to a Reynolds number range of 2,510,000 to 4,830,000 based on the mean aerodynamic chord of the full-span model (17.29 in.).

#### APPARATUS AND TESTS

The basic model is a  $\frac{1}{8}$ -scale model of the wing-fuselage combination of a transport airplane with the windshield discontinuity completely faired out. The scale of the model was large to facilitate accurate drag measurements of the windshield parts. Engine nacelles, landing gear, tail wheel, and tail surfaces were omitted so that the drag changes relative to the drag of the basic model might be as large as possible. The wing tips extended through the tunnel walls and were utilized as a convenient means of support. The wing is of steel covered with sheet aluminum, and the fuselage is mahogany with interchangeable nose sections for the various transport-type windshields. All surfaces were maintained aerodynamically smooth.

The windshields for the closed-cockpit tests were mounted on the basic model (figs. 1 and 2) in three interchangeable sections lettered N, M, and T that represent, respectively, the nose or windshield proper, the middle or hood, and the tail or hood fairing. Each

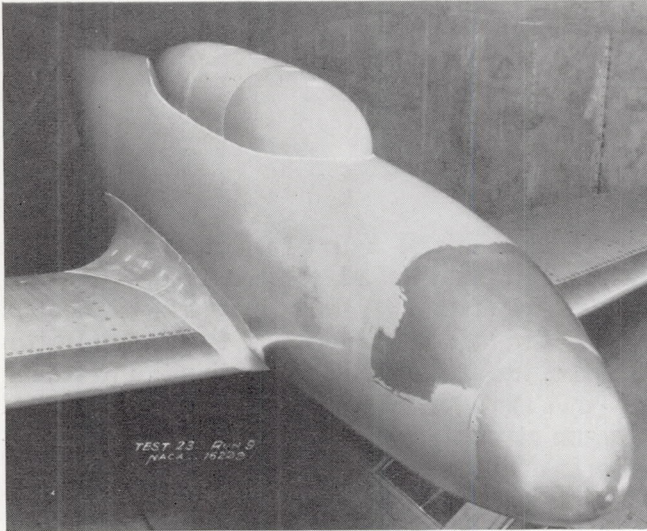


FIGURE 1.—Windshield combination 3-1-3 ready for testing in the tunnel.

windshield is designated by three numbers corresponding to the part numbers for N, M, and T shown in figure 3. For example, combination 1-1-3 has nose section 1, middle section 1, and tail section 3; 0 indicates that the middle section has been omitted and that the nose and the tail sections butt against each other. Most of the windshields are easily reproducible because of the regular geometric shapes on which they are based; windshield 4-0-3 is one-half the streamline body of

wing are approximately one-fourth full scale. For the transport-type windshields, the scale is one-eighth. The original transport-type windshield, the modifications to it, and the locations of these windshields are shown in figure 4.

## RESULTS

The drag results are presented as nondimensional coefficients. For the closed-cockpit types, the windshield drag coefficients are based on the windshield frontal area. For the transport types, the drag of the fuselage with various windshields is expressed as a fuselage drag coefficient based on the fuselage frontal area because the windshield area is not distinct from the fuselage frontal area.

For the closed-cockpit windshields, the windshield drag coefficient is

$$C_{D_{FW}} = \frac{\Delta D_W}{q F_W}$$

where

$\Delta D_W$  difference in drag between model with windshield and model without windshield

$F_W$  maximum cross-sectional area of windshield

$q$  dynamic pressure of free air stream ( $\frac{1}{2}\rho V^2$ )

For the transport-type windshields, the fuselage drag coefficient is

$$C_{D_{FF}} = \frac{\Delta D_F}{q F_F}$$

where

$\Delta D_F$  drag of complete model used less drag of wing; that is,  $\Delta D_F$  is drag of fuselage and includes interference of fuselage, windshield, and wing fillets

$F_F$  maximum cross-sectional area of fuselage

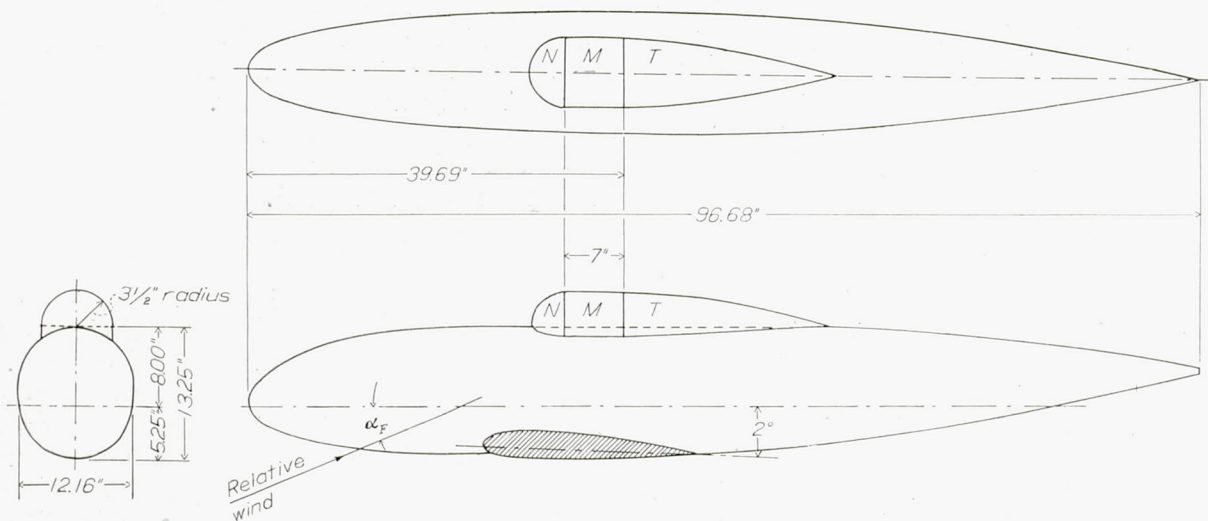


FIGURE 2.—Typical closed-cockpit windshield installation. Combination 1-1-3.

revolution, NACA form 111, fineness ratio 5, reported in reference 6. The windshields were all so located that the foremost part of the tail fairing was 39.69 inches behind the nose of the fuselage.

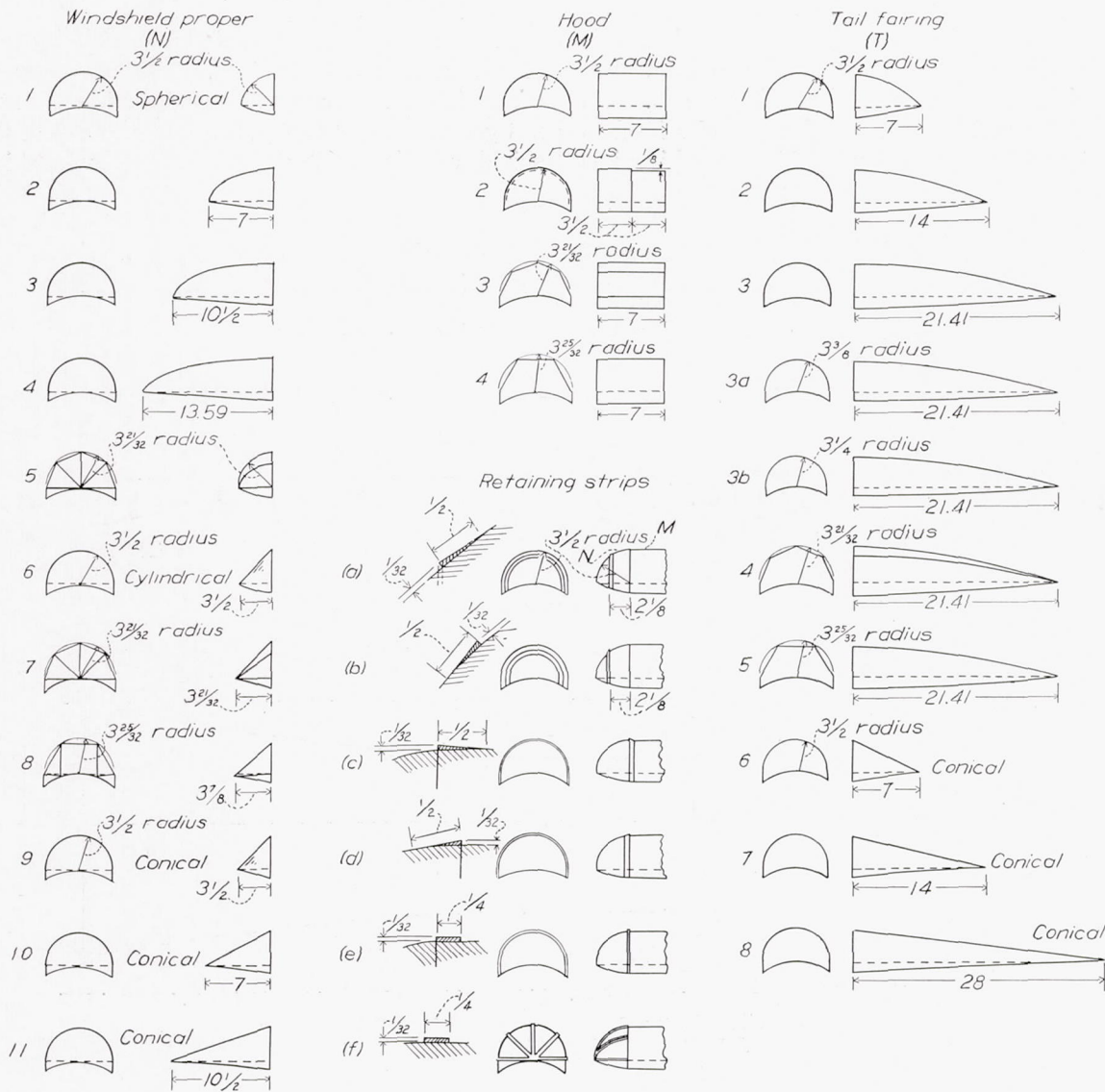
For the closed-cockpit windshields on one- and two-place airplanes, the windshield, the fuselage, and the

The pressure coefficient  $P$  is given by the equation

$$P = \frac{\Delta p}{q}$$

where

$\Delta p$  local static pressure at a point on windshield less static pressure of free air stream



All dimensions are in inches

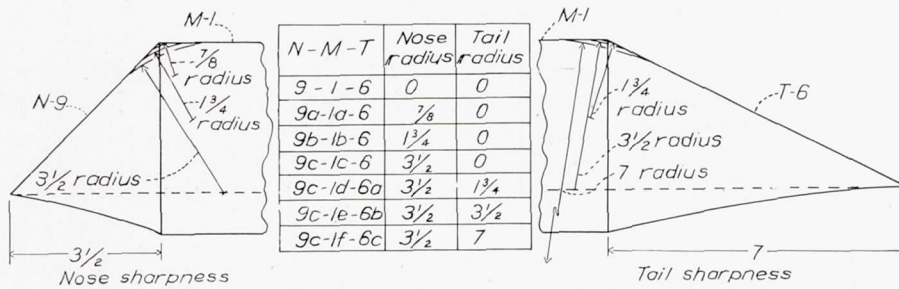


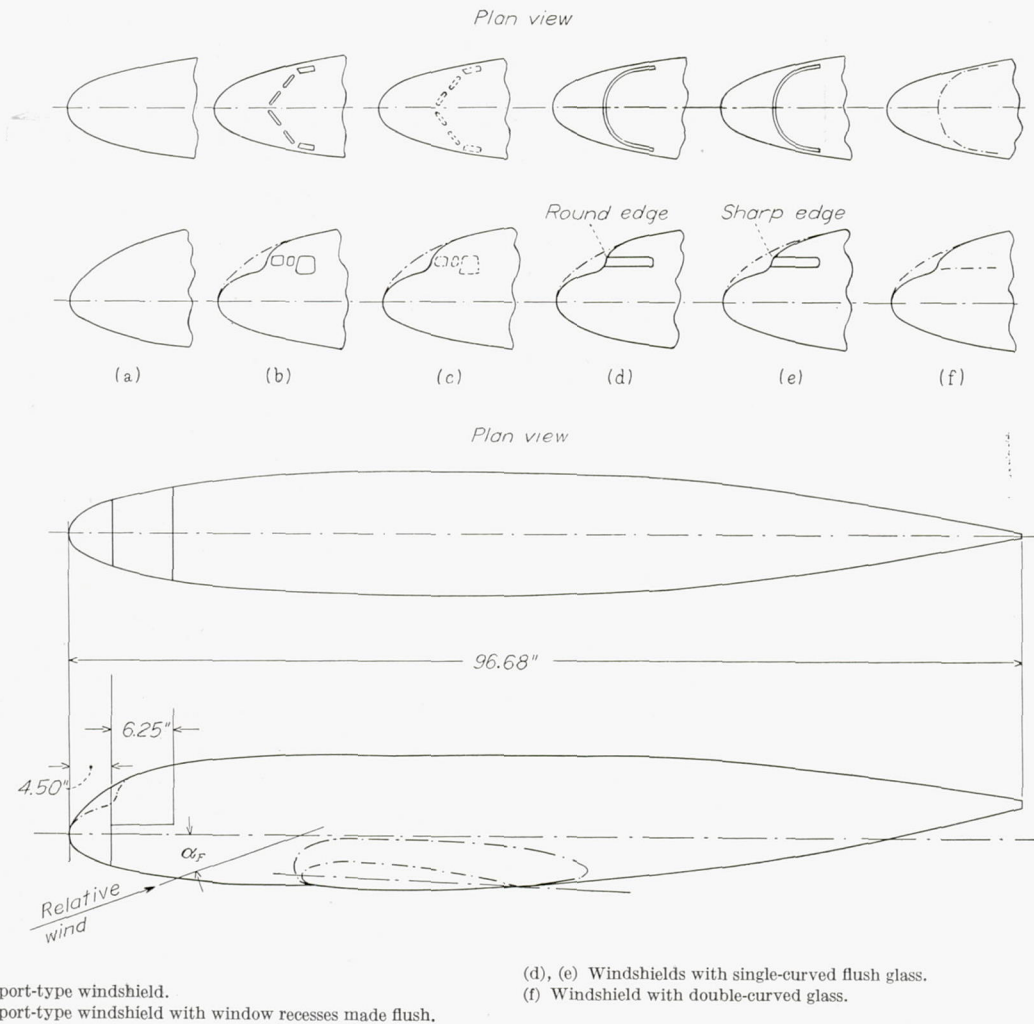
FIGURE 3.—Component parts of the closed-cockpit windshield combinations.

The results for the closed-cockpit windshields are presented as plots of  $C_{D_{FW}}$  of the windshield combination against the fuselage angle of attack  $\alpha_F$  for a sea-level speed of approximately 260 miles per hour (figs. 5 to 15). These plots show the effects of nose shape, nose length, tail length, radius at the juncture of windshield and hood, radius at the juncture of hood and tail, retaining strips, and steps for telescoping hoods. The variations of drag with angle of attack of the fuselage for the best and the poorest windshield combinations

The results for the transport-type windshields are presented as plots of  $C_{D_{FW}}$  against  $\alpha_F$  for a sea-level speed of 265 miles per hour (fig. 28).

#### PRECISION

The accuracy of the tests is best shown by the scatter of the experimental points. For the closed-cockpit windshields, the error in drag value is estimated to be not greater than 4 to 7 percent of the drag of the windshield and is smallest for the best windshields and



(a) Faired nose.

(b) Original transport-type windshield.

(c) Original transport-type windshield with window recesses made flush.

(d), (e) Windshields with single-curved flush glass.

(f) Windshield with double-curved glass.

FIGURE 4.—Transport-type windshields.

tested are shown in figure 16 for values of  $\alpha_F$  from  $-6^\circ$  to  $3.5^\circ$  for a sea-level speed of 137 miles per hour.

Cross plots showing the effects of nose length, tail length, radius at the juncture of windshield and hood, and radius at the juncture of hood and tail are shown in figures 17 to 22 for sea-level speeds of 229 to 381 miles per hour. The local pressures on two of the windshield combinations are shown as plots of the pressure coefficient  $P$  with Mach number  $M$  as a parameter for  $\alpha_F = -3.55^\circ, -1.79^\circ,$  and  $-0.03^\circ$  (figs. 23 and 24). The results for a few windshield combinations are plotted against  $M$  for  $\alpha_F = -3.55^\circ$  and  $-1.79^\circ$  to show the effect of compressibility on the drag (figs. 25 to 27),

largest for the poor windshields. For the transport-type windshields, the error is estimated to be not greater than 1 percent of the drag of the basic fuselage.

It is realized, of course, that the most important source of error in predicting full-scale characteristics from the model results probably is the difference in Reynolds number. Some transition effects may be of importance in the model tests; whereas the flow over an actual windshield will be affected by the propeller slipstream and by the character of other parts ahead of the windshield. For comparisons under the most unfavorable conditions, the results may apply at least qualitatively.

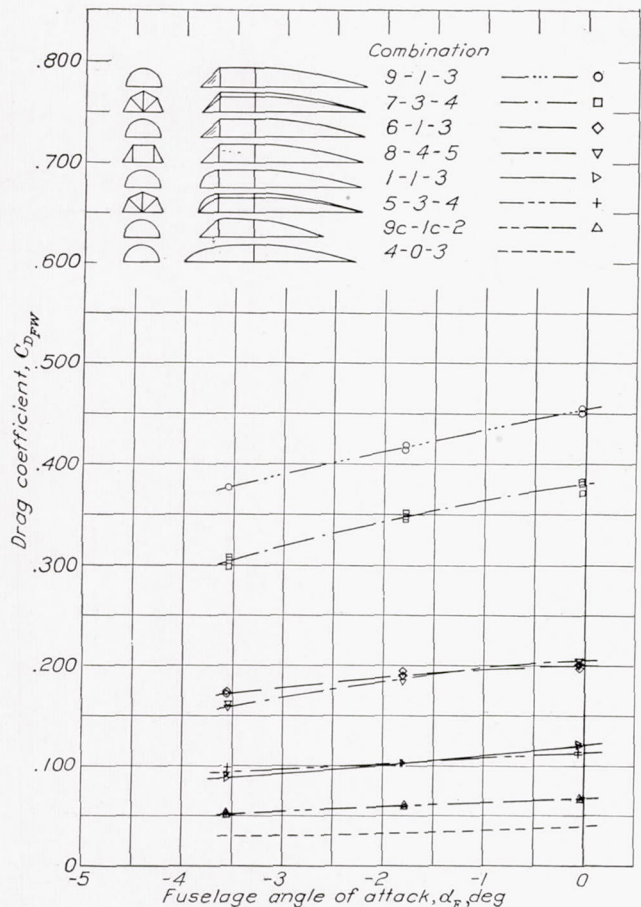


FIGURE 5.—Effect of nose shape of short length.  $M, 0.34; V, 260$  mph.

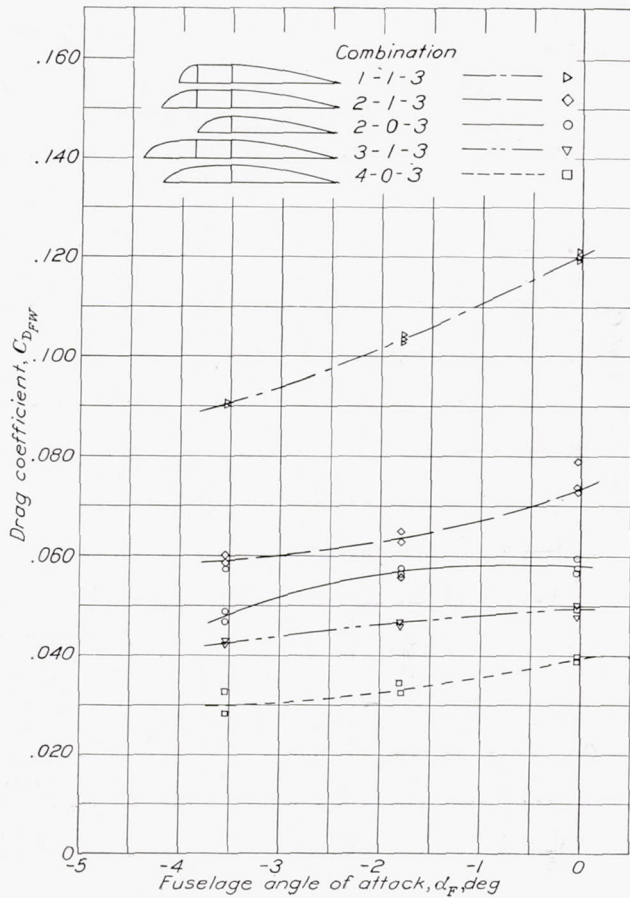


FIGURE 6.—Effect of nose length, streamline shape.  $M, 0.34; V, 260$  mph.

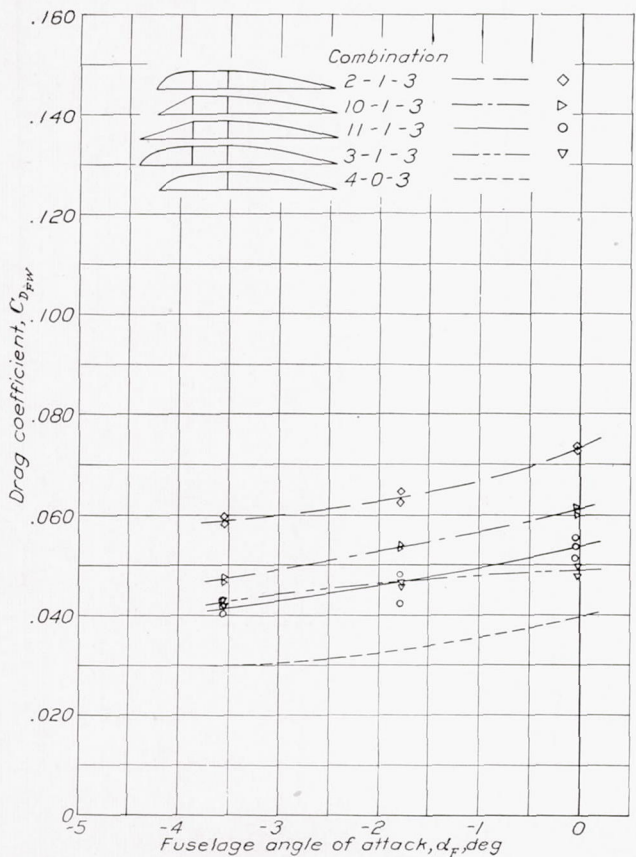


FIGURE 7.—Comparison between streamline and conical noses.  $M, 0.34; V, 260$  mph.

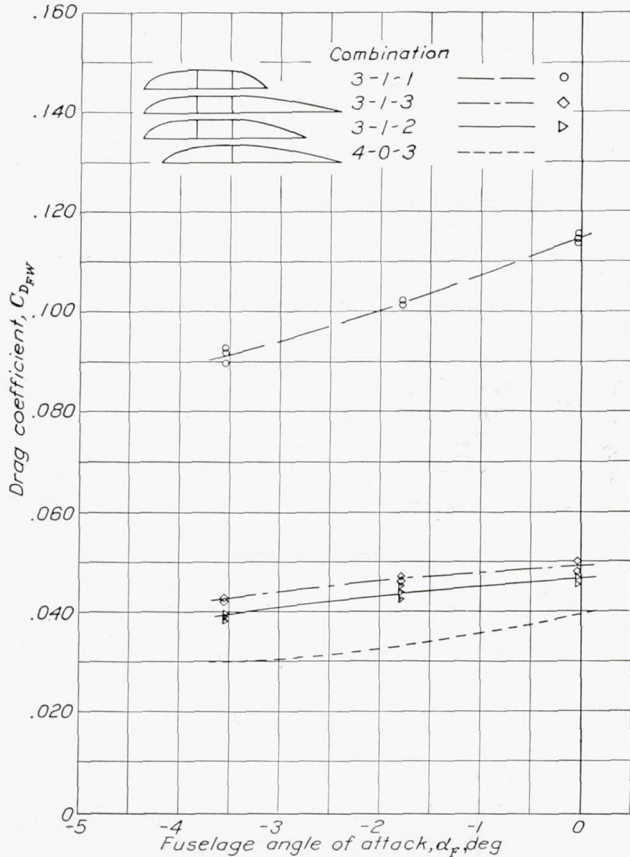


FIGURE 8.—Effect of tail length, streamline shape.  $M, 0.34; V, 260$  mph.

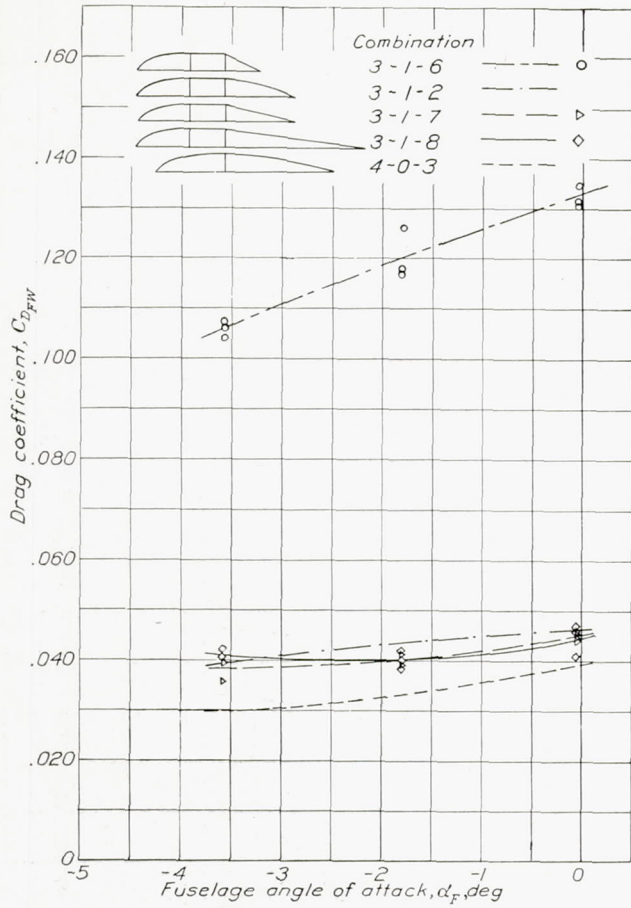


FIGURE 9.—Effect of tail length, conical shape.  $M, 0.34$ ;  $V, 260$  mph.

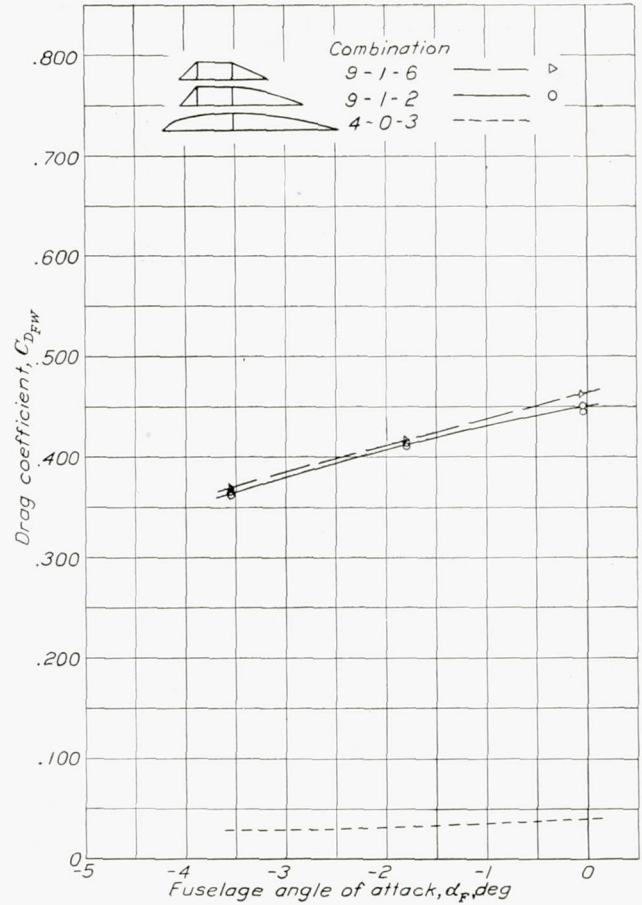


FIGURE 10.—Effect of tail length.  $M, 0.34$ ;  $V, 260$  mph.

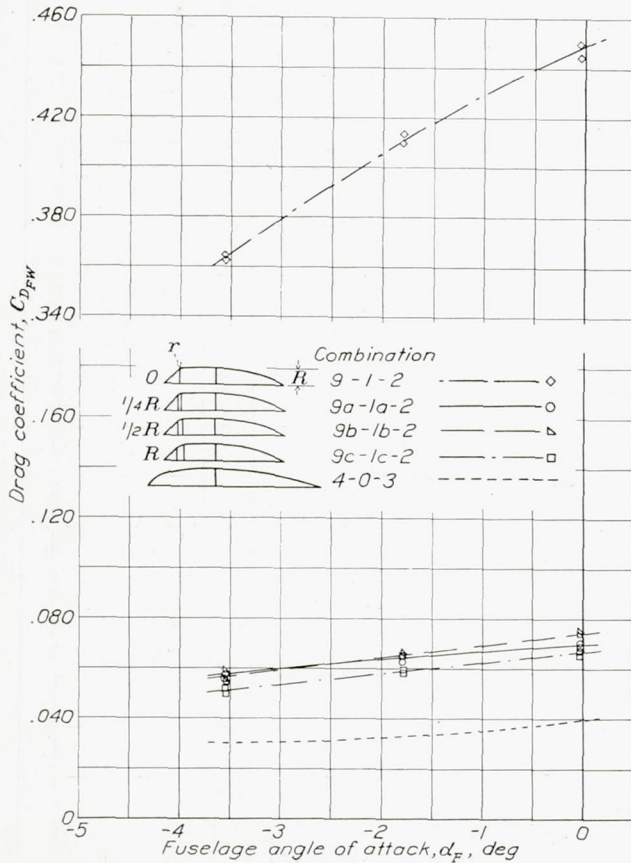


FIGURE 11.—Effect of radius at windshield-hood juncture.  $M, 0.35$ ;  $V, 265$  mph.

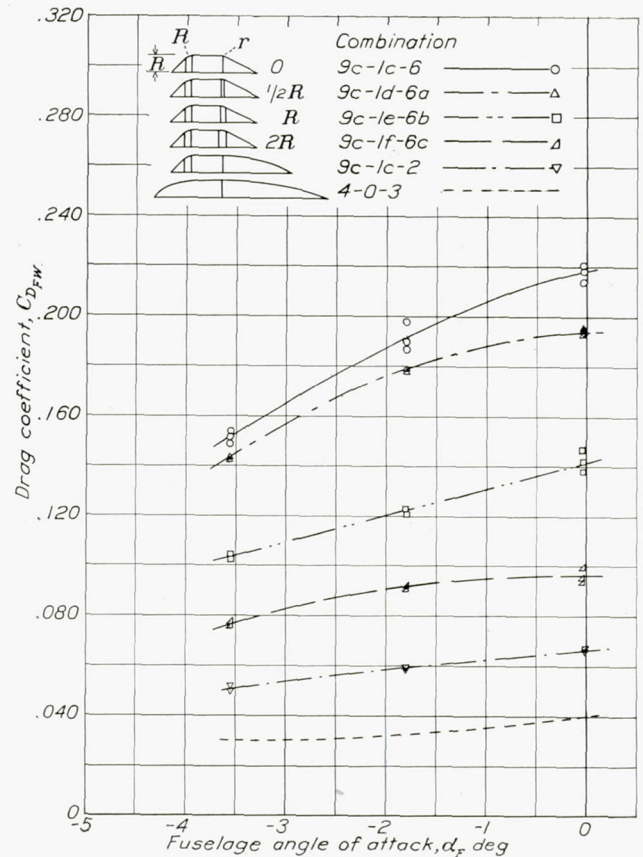


FIGURE 12.—Effect of radius at hood-tail juncture.  $M, 0.35$ ;  $V, 265$  mph.

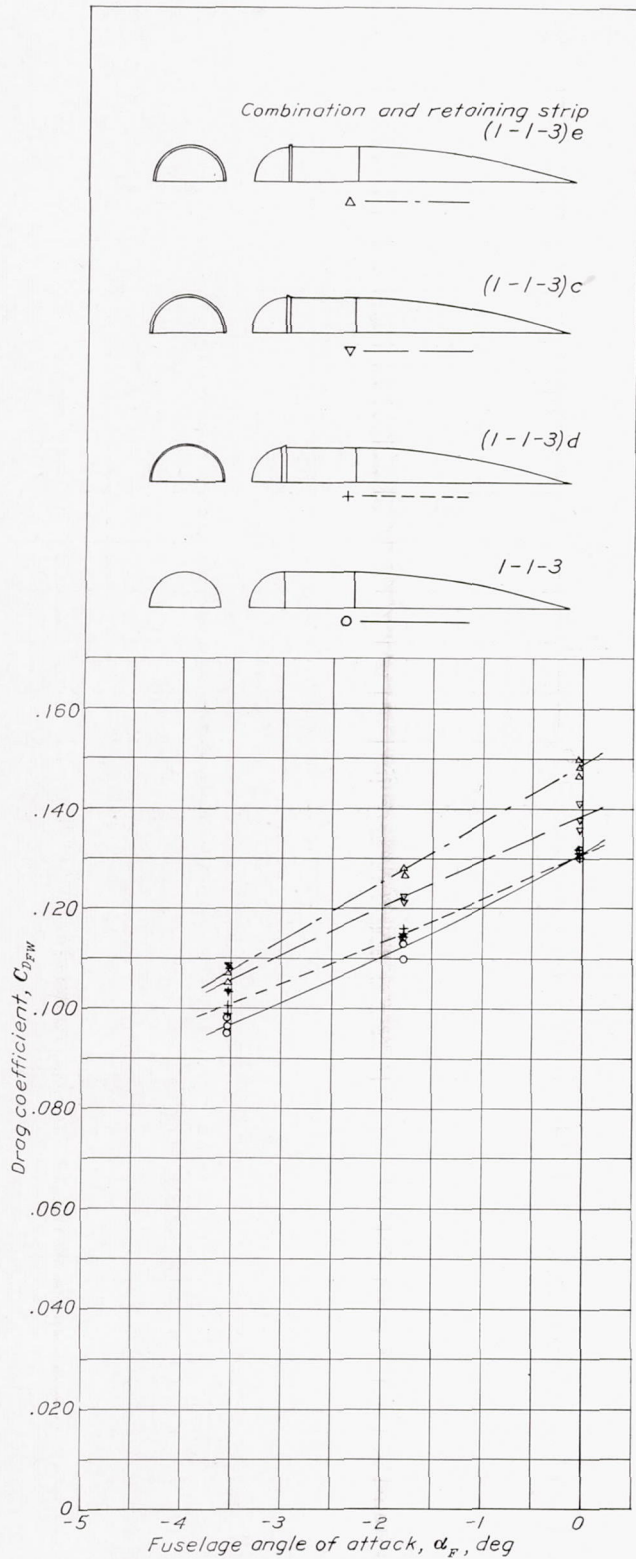


FIGURE 13.—Effect of retaining strips, combination 1-1-3.  $M, 0.34; V, 260$  mph.

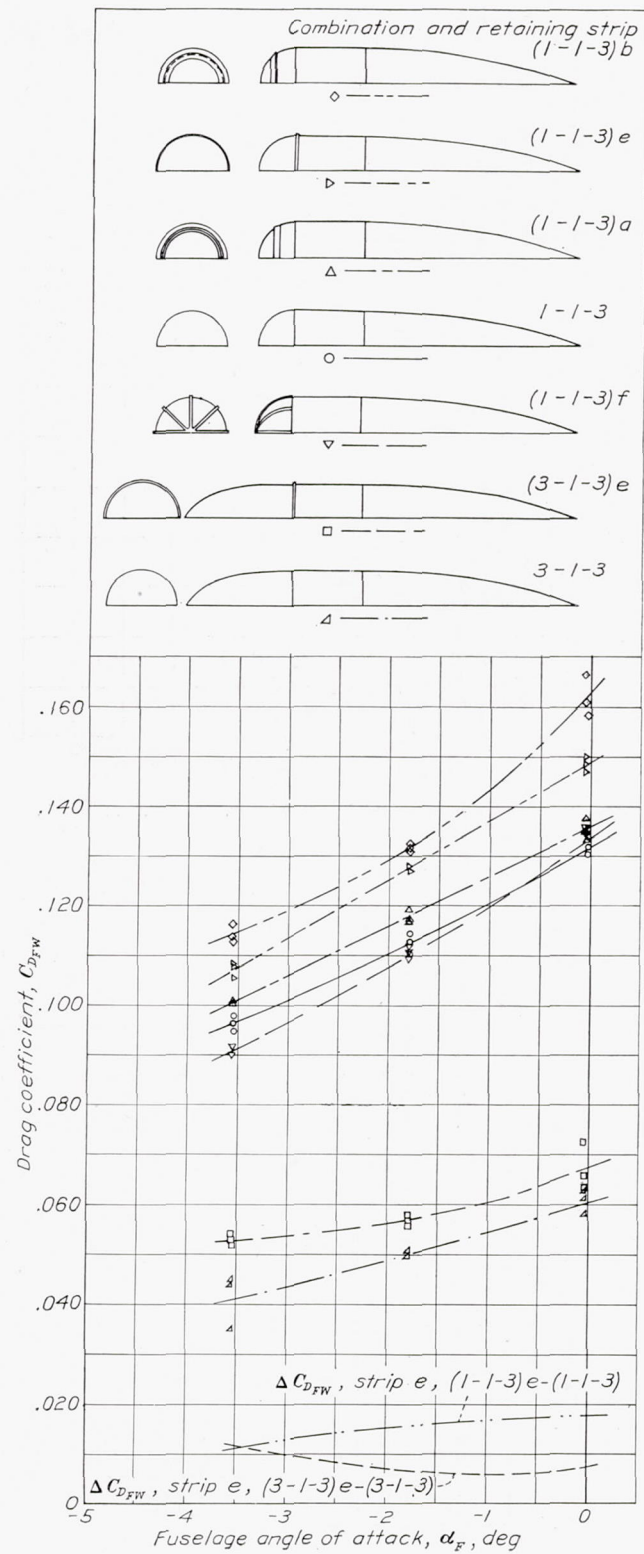


FIGURE 14.—Effect of retaining strips, combinations 1-1-3 and 3-1-3.  $M, 0.34; V, 260$  mph.

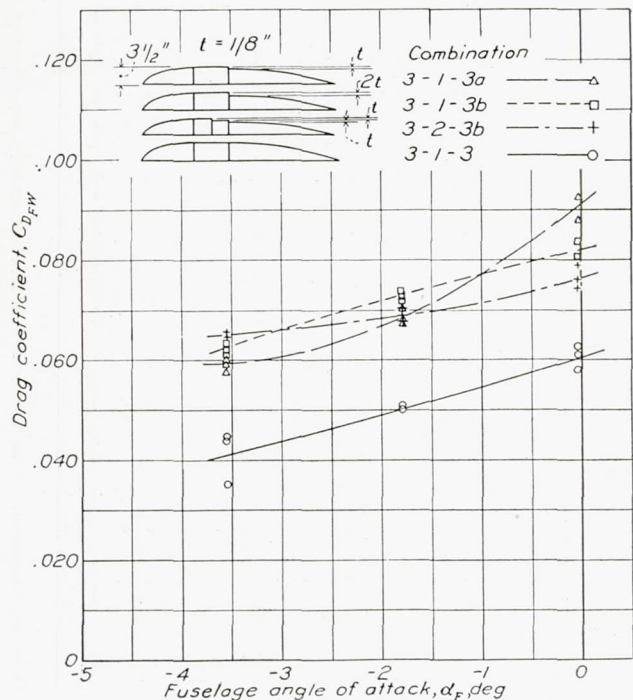


FIGURE 15.—Effect of steps for telescoping hoods.  $M$ , 0.34;  $V$ , 260 mph.

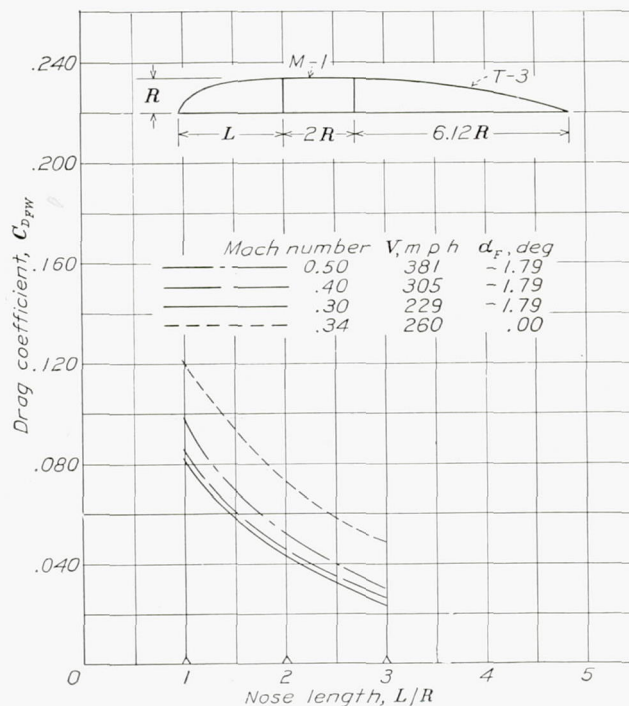


FIGURE 17.—Effect of nose length, streamline shape.

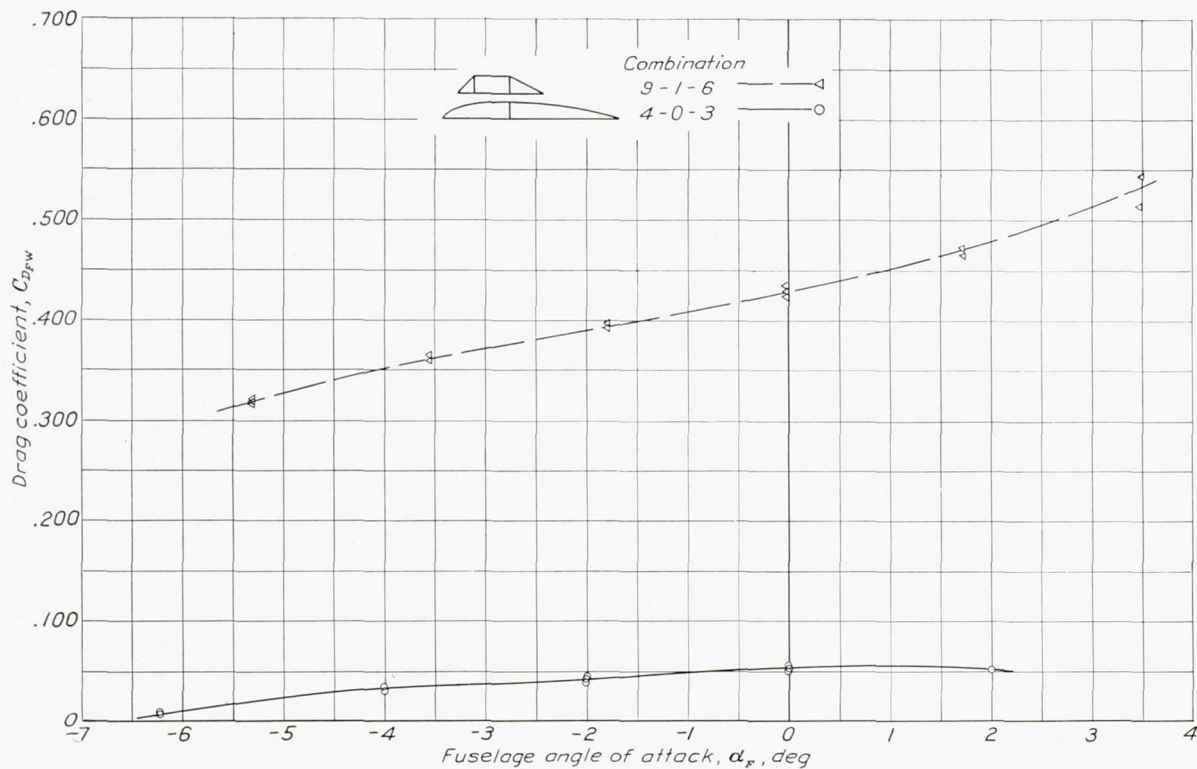


FIGURE 16.—Variation of drag with angle of attack.  $M$ , 0.18;  $V$ , 137 mph.

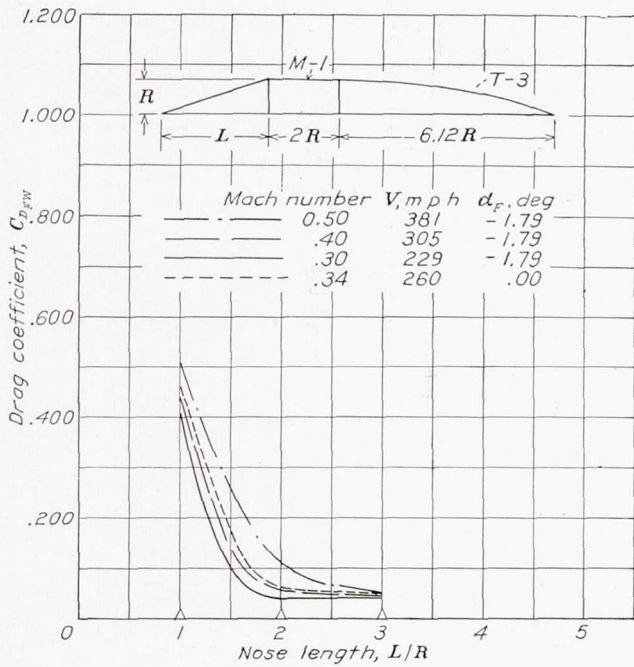


FIGURE 18.—Effect of nose length, conical shape.

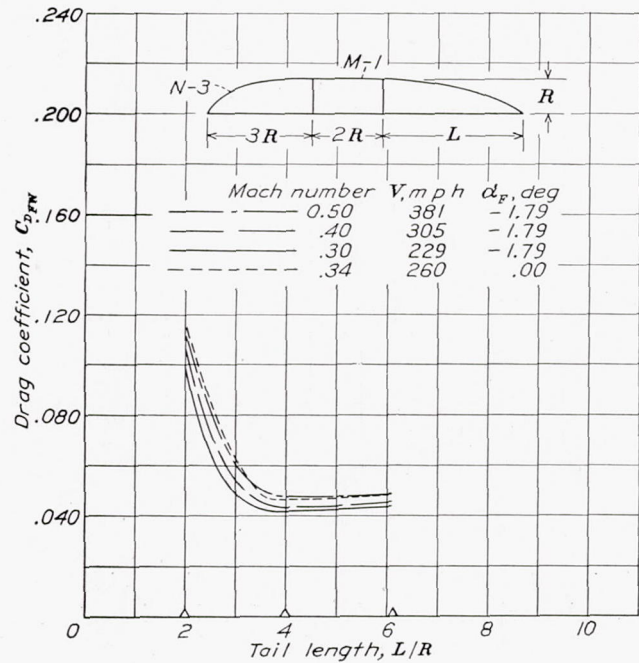


FIGURE 19.—Effect of tail length, streamline shape.

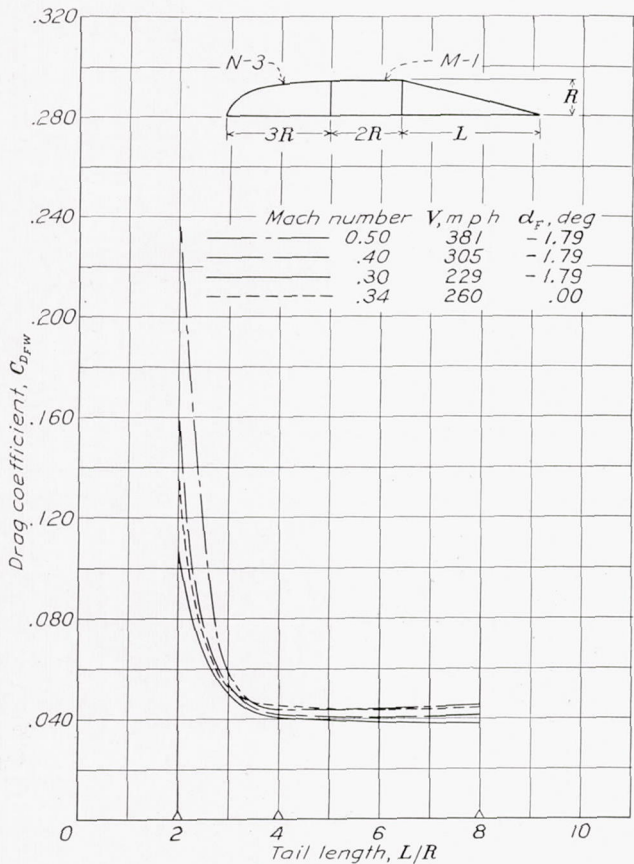


FIGURE 20.—Effect of tail length, conical shape.

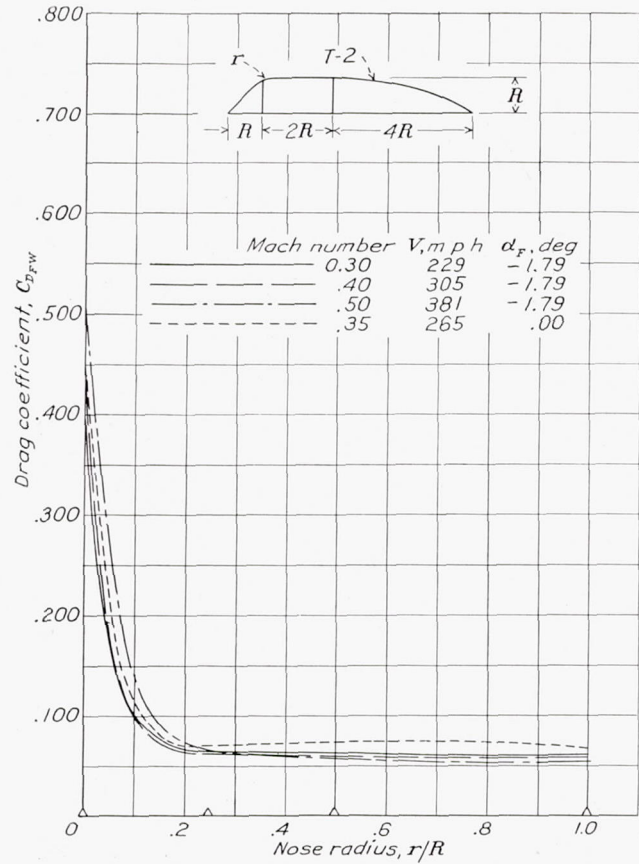


FIGURE 21.—Effect of radius at windshield-hood juncture.

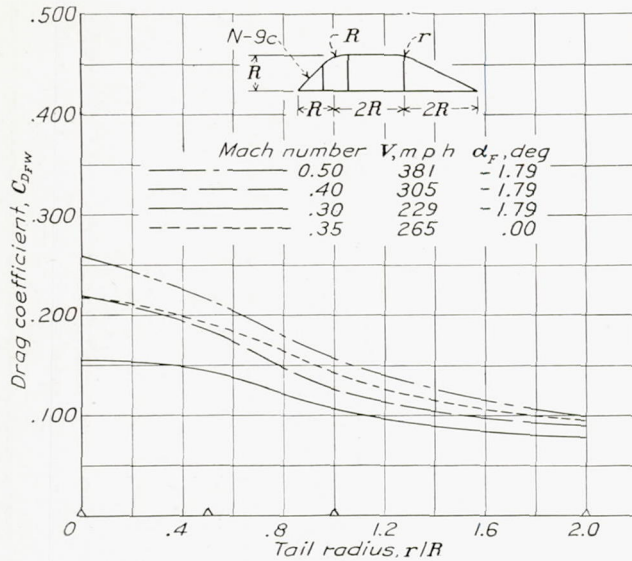


FIGURE 22.—Effect of radius at hood-tail juncture.

DISCUSSION

**Effect of nose shape.**—For nose sections with lengths approximately equal to the height of the windshield, the drag of combination 9-1-3 with a conical nose (fig. 5) is about the highest of any windshield tested and is approximately 15 percent of the drag of a small- or medium-

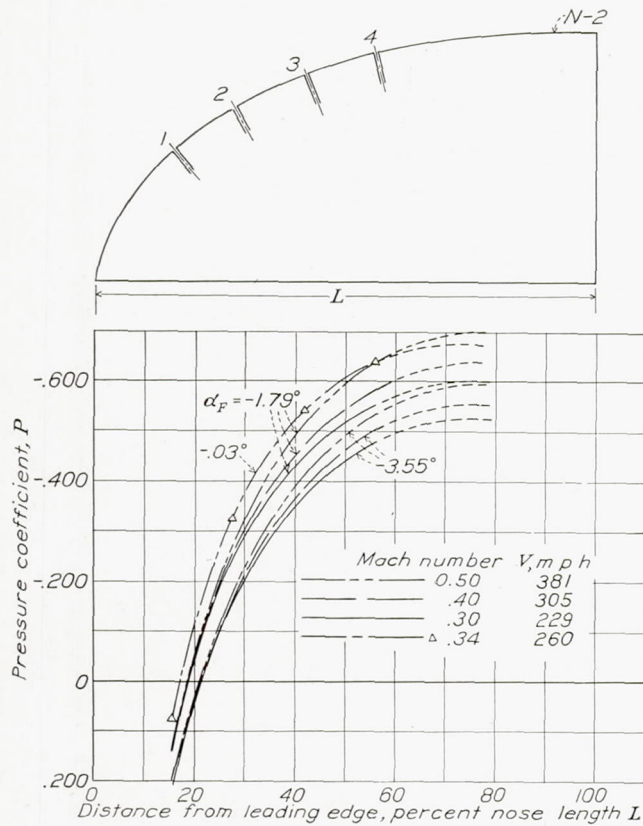


FIGURE 23.—Pressure distribution over streamline nose, medium length.

size airplane of average proportions. The conical nose is characterized by an obtuse angle between the nose and the hood that is of constant magnitude and continues around the complete transverse periphery of the windshield. That the drag depends on the sharp-

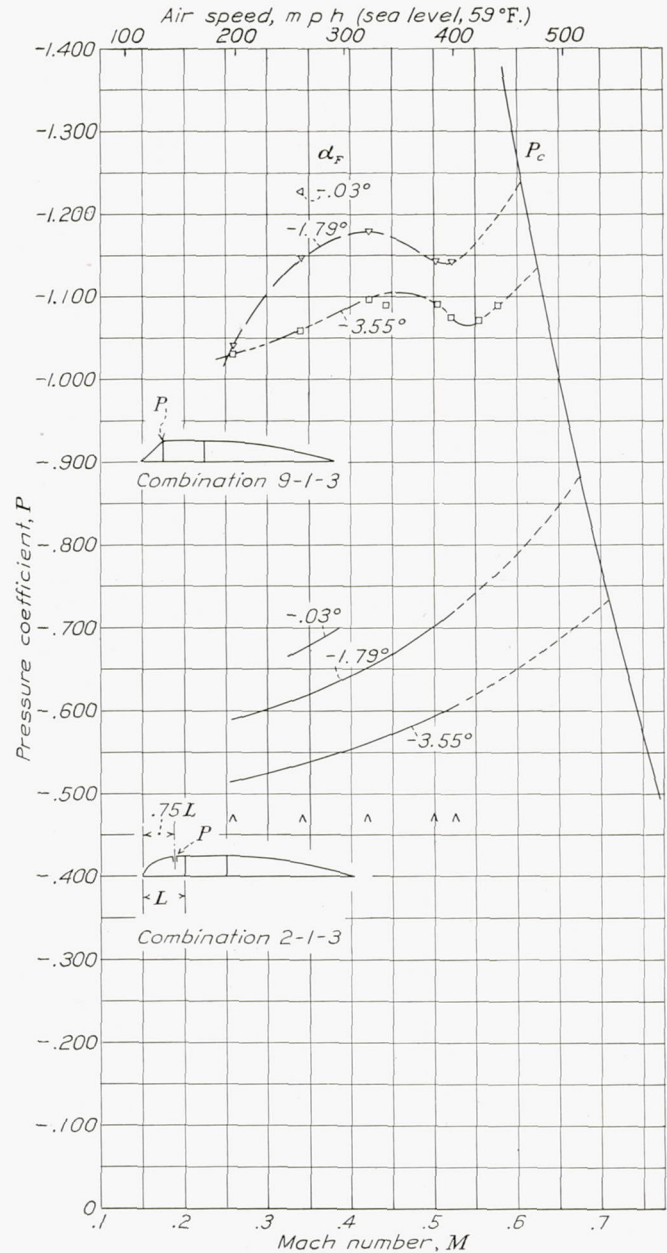


FIGURE 24.—Variation of peak negative pressure with speed for two windshields.

ness of this angle and the amount of windshield periphery with an angular break is shown by the fact that combination 6-1-3 with a cylindrical nose has about half the drag of combination 9-1-3 and that combination 1-1-3 with a spherical nose and no break has still less drag. Windshield drag depends largely on the longitudinal profile and only slightly on the transverse profile, as is shown by the general agreement in figure 5 of the curves for windshields having the same degree of edge sharpness but having semi-hexagonal or semi-octagonal transverse profiles instead of semi-circular. The drag of the streamline windshield 4-0-3 is the lowest of any windshield tested and is approximately 1 percent of the drag of a representative airplane. Rounding off the windshield corners, as in combination 9c-1c-2, is the best means of reducing the drag of a poor windshield. This effect is later discussed quantitatively.

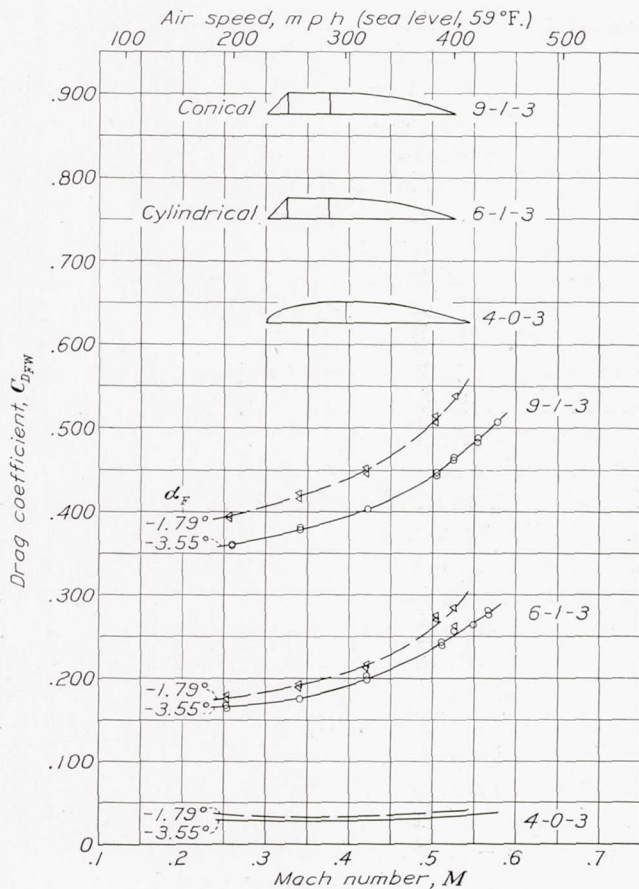


FIGURE 25.—Compressibility effect on windshield drag.

**Effect of nose length.**—The variation of windshield drag with length is somewhat similar for streamline noses and for conical noses, as shown by figures 6 and 7; the drag of the windshields progressively decreases as the length of the nose increases. The cross plots in figures 17 and 18 indicate that the optimum nose length for a conical-nose windshield is about  $2R$  for sea-level speeds up to 300 miles per hour and is greater than  $3R$  for higher speeds, that the length of a streamline-nose windshield should be greater than  $3R$ , and that the drag of a streamline-nose windshield longer than  $3R$  will be less than for a conical windshield.

**Effect of tail length.**—Figures 8 and 9 and the cross plots of figures 19 and 20 indicate that the length of both streamline and conical tail sections should be four times the height of the windshield. The optimum tail length, however, means little if a bad nose section is used, as a comparison of combinations 9-1-6 and 9-1-2 in figure 10 shows. There appears to be little choice between a long conical tail and a long streamline tail.

**Effect of radius at transverse junctures.**—Large reductions in the drag of a windshield with a short conical nose can be realized by rounding off the sharp edge at the windshield-hood juncture (fig. 11). The cross plots given in figure 21 indicate that the minimum effective radius is approximately 25 percent of the height of the windshield. Rounding off the sharp edge

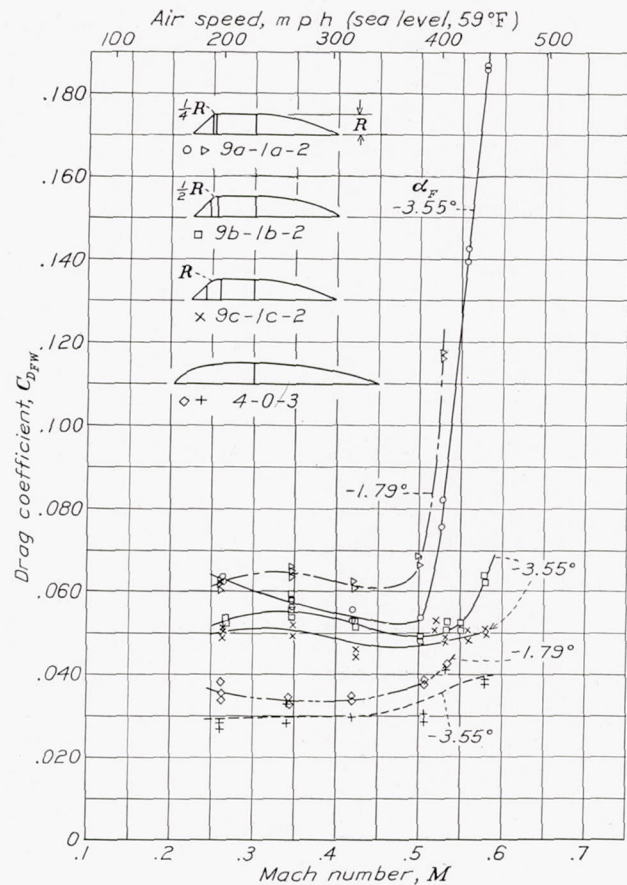


FIGURE 26.—Compressibility effect on windshields with various radii at nose-hood juncture.

to a greater radius decreases the drag very little at moderate speeds. A similar rounding off of the sharp transverse edges of the windshields shown in figure 5 will undoubtedly decrease the drag for these combina-

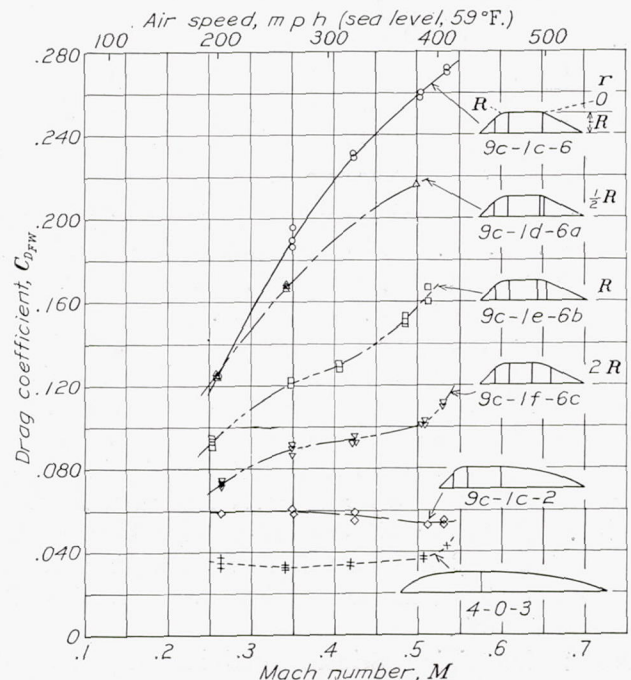


FIGURE 27.—Compressibility effect on windshields with various radii at hood-tail juncture.  $\alpha_F$ , -1.79°.

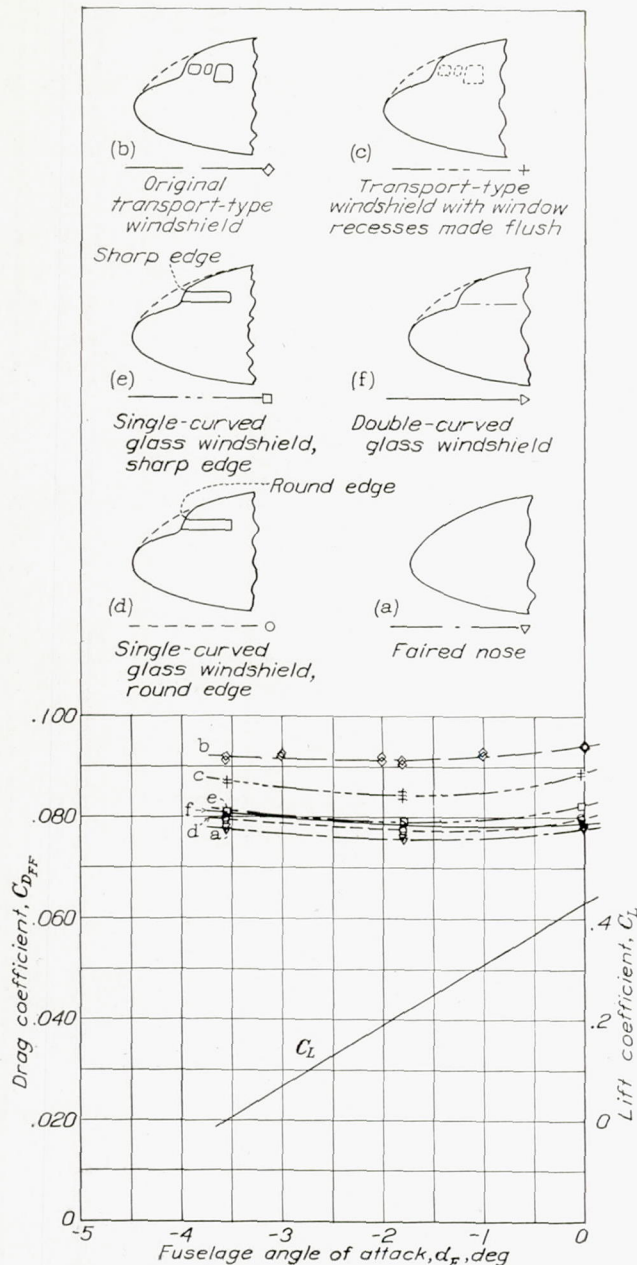


FIGURE 28.—Drag of fuselage with transport-type windshields.  $M$ , 0.35;  $V$ , 265 mph. tions also. The drag of these compromise windshields is, however, appreciably greater than that of windshield 4-0-3, which has a good basic shape.

Rounding off the sharp transverse edge at the hood-tail juncture of a rather short conical tail progressively decreases the drag as the radius is increased (fig. 12). The cross plots given in figure 22 show that the reductions in drag are much less than those obtained by a similar rounding off of the transverse edge on the nose section. Rounding off the sharp edge to a radius greater than  $2R$  does not appear to be important; greater reductions can be obtained by increasing the length of the tail.

**Effect of retaining strips.**—Retaining strips located at the windshield-hood juncture produce larger drag increments (figs. 13 and 14) for the spherical nose

(1-1-3)e than for the streamline nose (3-1-3)e. The drag of combination (1-1-3)f is shown in figure 14 to be lower than that of 1-1-3. This result is unexplainable but may be due to the fact that the distribution of pressure on a spherical shape is very sensitive to surface discontinuities; but, in any case, the differences in drag should be small. It is obviously advisable to make retaining strips as nearly flush with the glass as possible.

**Steps for telescoping hoods.**—Steps may increase the actual windshield drag from 25 to 50 percent, as shown by figure 15. The accuracy of these particular tests does not appear to be sufficient to indicate the relative drags of the various kinds of step. The detrimental effect of a cylindrical hood section may be seen in figure 6 by comparing combinations 2-1-3 and 2-0-3.

**Local pressures on windshields.**—Although the maximum negative pressures over nose 2 were not measured, extrapolation of the curves shown in figure 23 indicates that the peak negative pressure occurs at about 75 percent of the nose length back of the front of the nose. The curve of critical pressure coefficient  $P_c$  (the pressure coefficient at which the speed of sound is locally reached) against  $M$  (fig. 24) was derived from Bernoulli's equation for compressible flow. Extrapolation of the pressure coefficients of the two windshields tested to the curve of critical pressure coefficient  $P_c$  indicates that, for  $\alpha_f = -1.79^\circ$ , the local velocity of sound will be reached when  $M = 0.675$  (515 mph at sea level) for the streamline nose and when  $M = 0.605$  (460 mph at sea level) for the short conical nose. The drag of the windshield is expected to increase excessively at these speeds.

**Effect of speed.**—The drag of windshields having a short nose section with sharp transverse junctures increases very rapidly as the speed is increased, as is shown for two typical windshields in figure 25. The drags of windshields with fairly good nose and tail sections vary only slightly with speed, as does the drag of the best windshield 4-0-3 (figs. 26 and 27). Figure 26 shows the critical speed at which the drag rises abruptly for windshield 9a-1a-2 to be approximately 380 miles per hour at sea level, or  $M = 0.50$ , which indicates that small radii at the junctures may be satisfactory at low speeds but unsatisfactory at high speeds. An increase in the radius at the juncture to 100 percent of the windshield height prevented the occurrence of the compressibility shock within the range of these tests.

The effect of compressibility on the drag of a windshield with a short conical tail (fig. 27) decreases progressively as the transverse edge at the hood-tail juncture is rounded off to greater radii. Figure 22 indicates that a radius of  $2R$  is near the optimum value at medium speeds ( $M = 0.30$ ), but figure 27 shows that the compressibility effect is still great. The adverse effects can be reduced by using a longer tail, as is shown in figure 27 for combination 9c-1c-2. A general conclusion appears to be that poor windshields become relatively poorer as the speed increases.

**Transport-type windshields.**—The drag of the fuselage with the original transport-type windshield (b) is the highest and is an increase of 21 percent over the drag of the fuselage with the faired nose (a), as is shown in figure 28. The drag of the same windshield with the window recesses made flush (c) is 14 percent higher than the drag of the fuselage with the faired nose, which is a saving of 7 percent of the fuselage drag as a result of making the windows flush. The windshield with single-curved glass and a sharp edge at the juncture of window and roof (e) increased the drag about 4 percent of the basic fuselage drag; fairing this sharp edge (d) decreased the drag about 2 percent. The fuselage with double-curved glass (f) showed a drag increase varying from 2 to 3 percent of the basic fuselage drag. These results indicate that windshields using single-curved glass may have as low a drag as windshields using double-curved glass. This conclusion is probably true only for windshields with a generous fairing above the glass area, as in the present case. The sharp V-type windshields, (b) and (c), had higher drag coefficients as the speed was increased above 260 miles per hour; the other cabin windshields are not affected by compressibility, at least up to 440 miles per hour.

#### CONCLUSIONS

It is recognized that the results of this investigation are limited in their application by scale and slipstream effects and by the effects of parts that may be ahead of the windshield. The following conclusions drawn from these tests should nevertheless be useful as a general guide in design.

For closed-cockpit windshields:

1. The windshield drag for airplanes of small to medium size may account for 15 percent of the airplane drag or may be reduced to 1 percent.
2. Sharp junctures at the front of windshields are to be avoided. A radius of at least 25 percent of the windshield height should be used if the drag is to be kept low at medium speeds; a larger radius should be used for high-speed airplanes.

3. The optimum length for a conical windshield nose was twice the windshield height and, for a streamline nose, was more than three times its height; noses should be longer for higher speeds.

4. Tail fairings, whether conical or streamline, should be about four times as long as their height.

5. Steps for telescoping hoods increased the drag of a good windshield from 25 to 50 percent; retaining strips added measurably to the drag of a windshield.

6. Poor windshields became relatively poorer as speed was increased owing to compressibility effects and, in general, had lower critical speeds. The best windshields at low speed had the least compressibility effect over a wide speed range and had the highest critical speeds.

For transport-type windshields:

1. The windshield drag may account for 21 percent of the fuselage drag or may be reduced to 2 percent without completely fairing the windshield area.

2. Recessed windshield windows added 7 percent more to the fuselage drag than did flush windows.

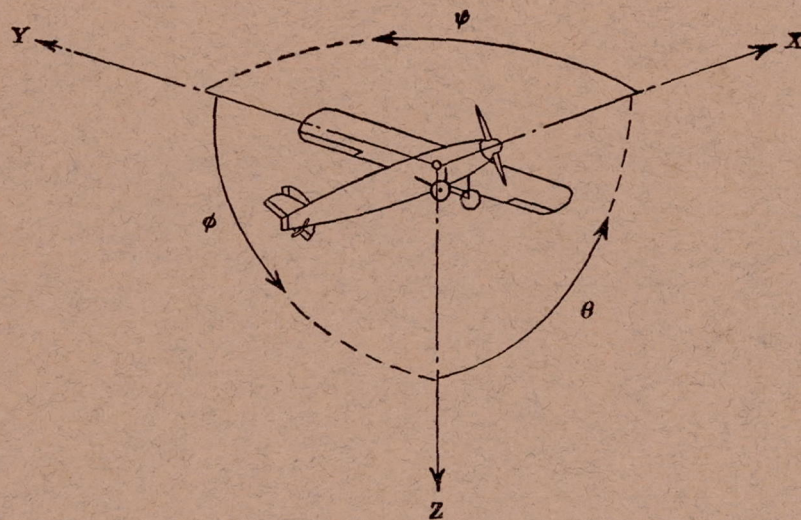
3. Sharp edges between windshield panels and cabin roof or sides added 2 to 14 percent to the fuselage drag.

LANGLEY MEMORIAL AERONAUTICAL LABORATORY,  
NATIONAL ADVISORY COMMITTEE FOR AERONAUTICS,  
LANGLEY FIELD, VA., *May 22, 1939.*

#### REFERENCES

1. Hartly, J. H., Cameron, D., and Curtis, W. H.: Note on Wind Tunnel Tests on the Design of Cabins. R. & M. No. 1811, British A. R. C., 1937.
2. Clay, William C.: Improved Airplane Windshields to Provide Vision in Stormy Weather. Rep. No. 498, NACA, 1934.
3. Serby, J. E.: Pilot's View in Cabin Aircraft. Aircraft Engineering, vol. X, no. 113, July 1938, pp. 219-220.
4. Jacobs, Eastman N.: The Reduction in Drag of a Forward-Sloping Windshield. T. N. No. 481, NACA, 1933.
5. Robinson, Russell G.: Sphere Tests in the N. A. C. A. 8-Foot High-Speed Tunnel. Jour. Aero. Sci., vol. 4, no. 5, March 1937, pp. 199-201.
6. Abbott, Ira H.: Fuselage-Drag Tests in the Variable-Density Wind Tunnel: Streamline Bodies of Revolution, Fineness Ratio of 5. T. N. No. 614, NACA, 1937.





Positive directions of axes and angles (forces and moments) are shown by arrows

| Axis              |             | Force<br>(parallel<br>to axis)<br>symbol | Moment about axis |             |                       | Angle            |             | Velocities                               |         |
|-------------------|-------------|--|-------------------|-------------|-----------------------|------------------|-------------|--|---------|
| Designation       | Sym-<br>bol |  | Designation       | Sym-<br>bol | Positive<br>direction | Designa-<br>tion | Sym-<br>bol | Linear<br>(compo-<br>nent along<br>axis) | Angular |
| Longitudinal..... | X           | X  | Rolling.....      | L           | Y→Z                   | Roll.....        | φ           | u  | p       |
| Lateral.....      | Y           | Y  | Pitching.....     | M           | Z→X                   | Pitch.....       | θ           | v  | q       |
| Normal.....       | Z           | Z  | Yawing.....       | N           | X→Y                   | Yaw.....         | ψ           | w  | r       |

Absolute coefficients of moment

$$C_l = \frac{L}{qbS} \quad C_m = \frac{M}{qcS} \quad C_n = \frac{N}{qbS}$$

(rolling)      (pitching)      (yawing)

Angle of set of control surface (relative to neutral position),  $\delta$ . (Indicate surface by proper subscript.)

#### 4. PROPELLER SYMBOLS

$D$  Diameter  
 $p$  Geometric pitch  
 $p/D$  Pitch ratio  
 $V'$  Inflow velocity  
 $V_s$  Slipstream velocity  
 $T$  Thrust, absolute coefficient  $C_T = \frac{T}{\rho n^2 D^4}$   
 $Q$  Torque, absolute coefficient  $C_Q = \frac{Q}{\rho n^2 D^5}$

$P$  Power, absolute coefficient  $C_P = \frac{P}{\rho n^3 D^5}$   
 $C_s$  Speed-power coefficient  $= \sqrt[5]{\frac{\rho V^5}{P n^2}}$   
 $\eta$  Efficiency  
 $n$  Revolutions per second, rps  
 $\Phi$  Effective helix angle  $= \tan^{-1}\left(\frac{V}{2\pi r n}\right)$

#### 5. NUMERICAL RELATIONS

1 hp = 76.04 kg-m/s = 550 ft-lb/sec  
 1 metric horsepower = 0.9863 hp  
 1 mph = 0.4470 mps  
 1 mps = 2.2369 mph

1 lb = 0.4536 kg  
 1 kg = 2.2046 lb  
 1 mi = 1,609.35 m = 5,280 ft  
 1 m = 3.2808 ft

NASA FILE COPY

Loan expires on last  
date stamped on back cover.

PLEASE RETURN TO  
REPORT DISTRIBUTION SECTION  
LANGLEY RESEARCH CENTER  
NATIONAL AERONAUTICS AND  
SPACE ADMINISTRATION  
Langley Field, Virginia